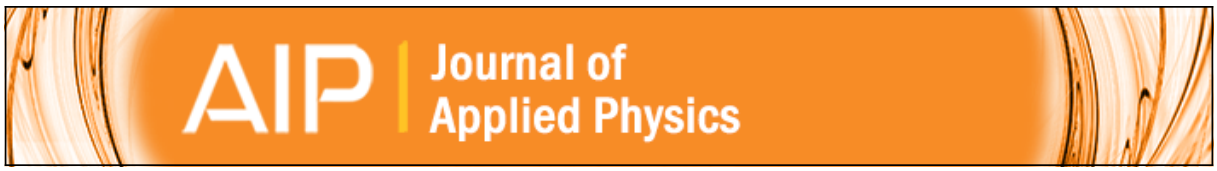

Temperature dependence of the electrical properties of hydrogen titanate nanotubes

Diego C. B. Alves, Fabio C. Fonseca, Frederico D. Brandão, Klaus Krambrock, and Andre S. Ferlauto

Citation: Journal of Applied Physics **116**, 184307 (2014); doi: 10.1063/1.4901589
View online: http://dx.doi.org/10.1063/1.4901589
View Table of Contents: http://scitation.aip.org/content/aip/journal/jap/116/18?ver=pdfcov
Published by the AIP Publishing

Articles you may be interested in

Influences of annealing temperature on structural characterization and magnetic properties of Mn-doped BaTiO3 ceramics
J. Appl. Phys. **112**, 013909 (2012); 10.1063/1.4733691

Novel approach for the synthesis of rutile titania nanotubes at very low temperature
J. Vac. Sci. Technol. B **29**, 021019 (2011); 10.1116/1.3554737

Electron spin resonance of defect-rich vanadium oxide nanotubes
J. Appl. Phys. **106**, 044313 (2009); 10.1063/1.3208066

In situ fabrication of alumina nanotube array and photoluminescence
Appl. Phys. Lett. **89**, 073114 (2006); 10.1063/1.2337160

Activation of oxide-ion conduction in KNbO 3 by addition of Mg 2+
Appl. Phys. Lett. **81**, 2899 (2002); 10.1063/1.1512957

[This article is copyrighted as indicated in the article. Reuse of AIP content is subject to the terms at: http://scitation.aip.org/termsconditions. Downloaded to] IP: 143.107.255.190 On: Wed, 07 Jan 2015 10:43:35

Temperature dependence of the electrical properties of hydrogen titanate nanotubes

Diego C. B. Alves,[1] Fabio C. Fonseca,[2] Frederico D. Brandão,[1] Klaus Krambrock,[1] and Andre S. Ferlauto[1]
[1]*Departamento de Física, Universidade Federal de Minas Gerais, Belo Horizonte, Minas Gerais 31270-901, Brazil*
[2]*Instituto de Pesquisas Energéticas e Nucleares, IPEN/CNEN-SP, 05508-000 São Paulo, Brazil*

(Received 9 September 2014; accepted 1 November 2014; published online 14 November 2014)

The temperature dependence of the electrical properties of hydrogen-rich titanate nanotubes (H-TNTs) in the 90–270 °C range was investigated by impedance spectroscopy. Three types of dominant conduction were found which depend on the previous thermal treatment of the samples. For untreated samples, at low temperatures ($T < 100\,°C$), electrical conductivity is relatively high ($>10^{-4}$ S/cm at $T \approx 90\,°C$) and is dominated by protonic transport within structural water molecules. For thermal annealing in inert atmosphere up to 150 °C, water molecules are released from the nanotube structure resulting in a dehydrated $H_2Ti_3O_7$ phase. Such phase has a low, thermally-dependent, electrical conductivity (10^{-8} S/cm at $T \approx 90\,°C$) with activation energy of 0.68 eV. For samples annealed up to 260 °C, loss of OH groups, and consequent generation of oxygen vacancies, occurs that result in the non-stoichiometric $H_{2(1-z)}Ti_3O_{7-z}$ phase. This phase has much higher conductivity (10^{-5} S/cm at $T \approx 90\,°C$) and lower associated activation energy (0.40 eV). The generation of oxygen vacancies is confirmed by electron paramagnetic resonance measurements at room temperature, which revealed the presence of single-electron-trapped oxygen vacancies. The activation energy value found is consistent with the thermal ionization energy of the oxygen vacancies. Such defect formation represents the initial stage of the phase transformation from titanate to TiO_2 (B). X-ray diffraction and Raman spectroscopy measurements also support such interpretation. © *2014 AIP Publishing LLC*. [http://dx.doi.org/10.1063/1.4901589]

INTRODUCTION

Hydrogen (and sodium) titanate nanotubes (TNTs) are filamentary structures that can be easily produced from alkaline treatments of titanium dioxide powders, as proposed originally from Kasuga *et al.*[1] They have interesting physicochemical properties, such as high specific surface area (as high as 300 m^2/g), high water retention ability, and excellent cation exchange capability.[2,3] Earlier studies on TNTs synthesis and characterization have shown that their structure and composition can be controlled by either adjusting synthesis parameters, such as solvothermal temperature, or using post-treatments, such as cation exchange or thermal annealing.[3] The relative content of Na and H in TNTs can be easily controlled by exchanging Na cations, which are originally present from the alkaline process, with protons in an acid treatment. As a result, the composition of TNTs can vary and a general formula is given by $Na_xH_{2-x}Ti_3O_7{:}H_2O$, where x indicates the relative amount of sodium. Na-rich and H-rich TNTs can have distinct properties especially in terms of thermal stability and water retention.[4]

In recent years, TNTs have become target of many studies in fields such as catalysis,[3] hydrogen sensing,[5] and hydrogen storage.[6,7] In particular, several works have reported that TNTs samples have high protonic conductivity under high relative humidity (RH) conditions,[2,8] and such feature has stimulated the use of TNTs as fillers in nanocomposite membranes for both hydrogen and ethanol-fueled proton exchange fuel cells.[9–11] TNTs are easily hydrated and can store within their multilayers a large amount of intercalated water that has strong influence on the protonic conductivity at low temperatures ($T < 100\,°C$). Although, water-based protonic transport within TNTs has been readily recognized, studies on their transport properties under low humidity conditions have been limited. From impedance measurements, Thorne *et al.* determined the temperature (T) dependence of the conductivity of hydrogen-rich TNT (H-TNT) pellets.[12] They observed an abrupt drop of around two orders of magnitude in conductivity at $T \approx 120\,°C$, which was attributed to a transition from a protonic transport at low T to electronic transport at higher T.[12] Hu *et al.* also observed a conductivity drop in a similar temperature range.[13] However, in these works, the conductivity was measured during heating, and the fact that structural modification of the TNTs might be occurring due to the thermal annealing was ignored. Such effect cannot be neglected since several studies have shown that TNTs, in particular H-TNTs, can undergo significant structural transformation when heated even at relatively low temperatures.[4,14] Therefore, in the present work, we performed a careful study of the temperature dependence of H-TNT in order to identify and separate contributions from protonic and electronics transport and investigate the effect of structural transformation on their electronic transport properties.

EXPERIMENTAL METHODS

Synthesis of hydrogen-rich titanate nanotubes was performed by a reflux method according to procedure

 © 2014 AIP Publishing LLC

[This article is copyrighted as indicated in the article. Reuse of AIP content is subject to the terms at: http://scitation.aip.org/termsconditions. Downloaded to] IP: 143.107.255.190 On: Wed, 07 Jan 2015 10:43:35

previously reported.[5] 500 mg anatase TiO_2 powder (Sigma Aldrich - 99%) was refluxed in 200 ml of NaOH (10 M) aqueous solution under vigorous magnetic stirring for 24 h. The resulting material was washed with a diluted solution of HCl (0.1 M), until pH = 3 was reached, and then washed with deionized water until a neutral suspension was recovered. After overnight drying in a furnace at 60 °C, the resulting material consisted of a white powder.

Phase identification was conducted by powder X-ray diffraction (XRD) using Cu K_α radiation ($\lambda = 1.54$ Å) with scattering angle (2θ) ranging between 4 and 80° (step size of 0.05°). Raman spectroscopy was performed in the range between 200 and 1100 cm^{-1} using a solid state laser ($\lambda = 532$ nm) as excitation source (DeltaNu). Electron paramagnetic resonance (EPR) measurements were carried out in a custom-build spectrometer working at X-band having commercial cylindrical cavity (Bruker), klystron source (Varian), and magnet (Varian, 0–800 mT). Electrical properties were studied by impedance spectroscopy measurements of H-TNT pellets, prepared from 200 mg of H-TNT powder, which were pressed (axial pressure of 13 MPa) without any binder. The resulting pellets had thickness of ~0.8 mm and diameter of 1.3 cm. Highly conductive silver ink was painted onto opposite parallel surfaces of the pellets and dried in air at 80 °C for 1.5 h to form the electrical contacts. Pellets were placed in a gas tight sample holder with a type K thermocouple and Pt contact leads that was inserted inside a tubular furnace.[15] Impedance measurements were performed under Argon flow (oxygen concentration ~5 ppm) by using a Solartron 1260 impedance analyzer over a frequency range of 10–10^7 Hz and 200 mV ac amplitude.

RESULTS

The electrical properties of TNT-H pellets were determined in two measurement sessions that last several hours each. In both sessions, the temperature was increased stepwise in a sequence of several fixed plateaus. At each plateau, impedance spectra were regularly taken in fixed time intervals. Impedance spectra were also collected during the unforced cooling of the samples. The original idea was to capture the dynamic effects of water desorption and distinguish the protonic contribution mediated by the adsorbed and/or intercalated water molecules to the overall conductivity from electronic transport.

Figure 1 shows impedance spectra measured at 88 °C for samples having different thermal histories. Fig. 1(a) depicts a spectrum taken in the beginning of one of the measurement sessions, whereas Figs. 1(b) and 1(c) show spectra of samples subject to complete measurement sessions in which the samples were heated up to 160 °C and up to 270 °C, respectively. The spectra consist of a depressed semi-circle at high frequency and a low frequency component that corresponds to electrode polarization. They were analyzed by using the equivalent circuit model shown in Fig. 1(d), whereby CPE corresponds to a constant-phase element. We have chosen to use such simple model in order to be able to provide a useful comparison between dozens of spectra taken at different temperatures. The obtained adjusts are depicted as solid lines

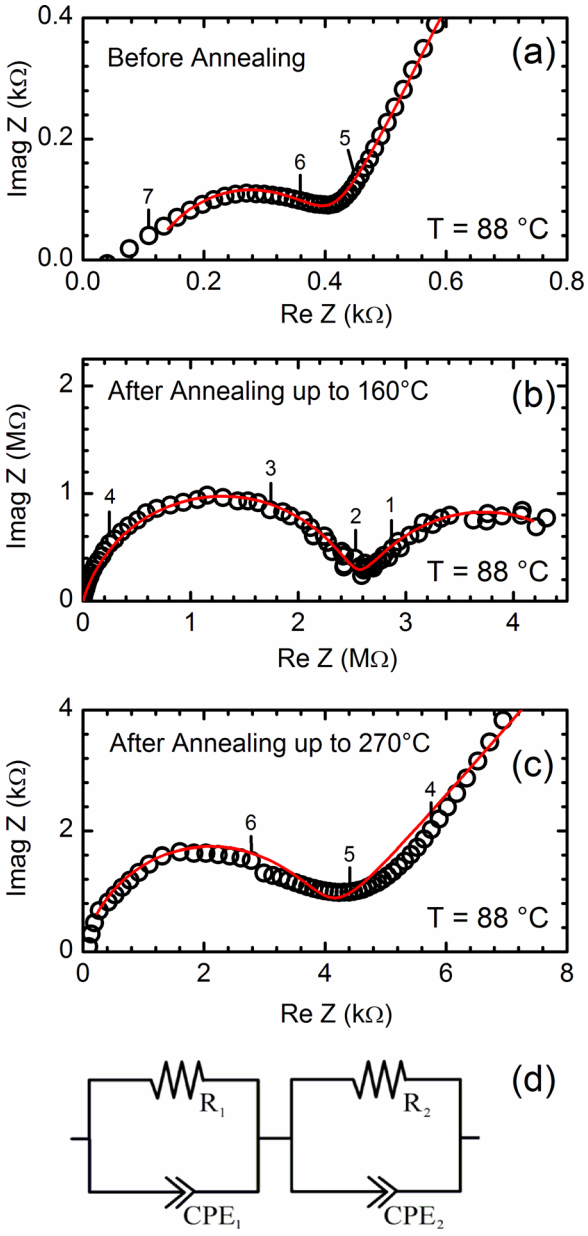

FIG. 1. Representative spectroscopic impedance spectra taken at T = 88 °C (circles). (a) Impedance spectrum taken before any thermal annealing and after thermal annealing at a maximum of (b) 160 °C and (c) 270 °C. Numbers indicate the logarithm of frequency. The spectra were adjusted (red curves) using the equivalent circuit model depicted in (d) in which the elements (resistor, R, and critical phase element, CPE) indexed with 1 correspond to the sample properties and the one indexed with 2 corresponds to the electrodes response. For the spectra in (a), the equivalent circuit also includes inductor in series to account for parasitic inductance.

in Fig. 1. The conductivity of the samples, σ, was determined from the best fit value for the sample "bulk" resistance (R_1) and the sample geometrical factor. By comparing the spectra in Figs. 1(a)–1(c), large differences in the absolute values of R_1 can be observed. Since these spectra were all measured at the same temperature (T = 88 °C), such differences in conductivity arise only from differences in the samples thermal history. This indicates that thermal annealing of TNT-H induces significant changes in the transport properties of TNT-H. Such relation was further investigated as described next.

[This article is copyrighted as indicated in the article. Reuse of AIP content is subject to the terms at: http://scitation.aip.org/termsconditions. Downloaded to] IP: 143.107.255.190 On: Wed, 07 Jan 2015 10:43:35

Figure 2(a) depicts the time evolution of the measurement temperature (solid line) and of the conductivity (symbols), as obtained from the impedance analysis, during the heating up stage of the longest measurement, performed up to 260 °C. For the low temperature plateaus (T < 150 °C), large conductivity drops can be observed at constant temperature. At T = 150 °C, the conductivity reaches a minimum of around 2.6×10^{-7} S/cm and upon further temperature increase, the conductivity starts to increase continuously up to the maximum measured temperature, reaching $\sim 10^{-3}$ S/cm at T = 270 °C. In the shortest measurement session, the same temperature time profile was followed, but only up to 160 °C, and very similar conductivity values were obtained for the heating stage. The heating endpoints of both measurements are indicated in Fig. 1(a). In both measurement sessions, the sample's conductivity was also determined during the unforced cooling.

The temperature dependence of the conductivity during heating and during cooling for the two measurements can be directly observed in Fig. 2(b). The first thing to consider in this plot is the relatively high values of conductivity ($>10^{-4}$ S/cm) found at T < 100 °C in the beginning of the measurements. Such high values can be attributed to Grottuss-like protonic transport occurring within intercalated and/or adsorbed water molecules, since it is well know that titanate nanotubes can withhold significant amount of weakly physisorbed and intercalated (crystallographic) water molecules.[4,14,16] Similar values of conductivity for TNT were found in measurements at 100% RH by Kasuga *et al.*,[1] which were attributed to protonic conduction, and even higher values were obtained for TNT functionalized with phosphonic or sulphonic groups.[2,10]

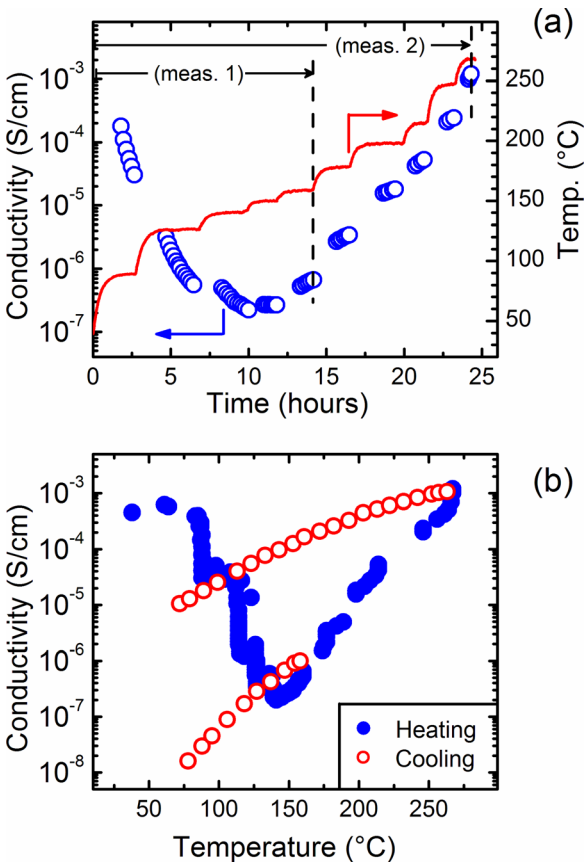

FIG. 2. (a) Schematic plot depicting the evolution of the annealing (and measurement) temperature and the measured "bulk" conductivity versus time upon heating during the two measurement sessions. Each cluster of conductivity data points corresponds to a period of fixed temperature plateaus. (b) The dependence of sigma on temperature upon heating and subsequent cooling for the two measurement sessions up to T = 160 °C and T = 270 °C.

The decrease in σ when T is increased from about 80 to 150 °C can be attributed to the release of crystallographic and/or physisorbed water molecules from the nanotube structure. In fact, detailed NMR and thermal analysis studies have shown that significant water loss occurs within this range of temperature.[14,16] Upon heating, the dehydration follows a sequence that starts with the loss of crystallographic water molecules according to the following reversible reaction:[16]

$$H_2Ti_3O_7 \cdot xH_2O \longleftrightarrow H_2Ti_3O_7 + xH_2O. \quad (1)$$

Therefore, the temperature dependence shown in Fig. 2 clearly demonstrates that for low temperature, protonic-type conduction is responsible for the relative high values of conductivity and that such contribution is diminished and almost disappears upon heating due to the release of water molecules from the titanate structure. Similar drop in conductivity has been observed before.[12,13] It is worth noting that in both previous works, there was an initial increase in conductivity for T up to ~120 °C, which can be related to the thermal activation of the protonic conduction.[12,13] In our measurements, such initial thermally activated increase in the protonic contribution was also observed but only for temperatures lower than 80 °C (not shown). This difference probably occurs because water desorption was enhanced in our measurements, made in inert atmosphere, as compared to the measurements performed in Refs. 12 and 13, which were done in air. We have chosen to focus our analysis on T above 80 °C to identify the point of transition between the protonic and electronic conduction regimes on H-TNT structures with better accuracy and likewise the associated phase transformation dynamics.

Upon cooling from T = 160 °C, the conductivity values do not follow the same trend as the values obtained upon heating. Such irreversibility is also explained by the loss of adsorbed water molecules that result in an almost complete disappearance of the protonic transport contribution. In fact, such disappearance is reflected in the four order of magnitude decrease in conductivity at T ≈ 90 °C for measurements before and after the heating up to 160 °C [Fig. 2(b)].

The conductivity values obtained for measurements above 150 °C can be attributed mainly to the intrinsic transport of titanate nanotubes and not from water-based protonic transport. The increase in conductivity observed upon heating above 150 °C suggests a thermally activated transport, as expected for electronic transport in transition metal oxide semiconductors.[17] However, further changes on the titanate nanotubes might also be occurring with increasing measuring temperature, and thus a better way to investigate the temperature dependence of conductivity in these materials is to measure the conductivity upon cooling after the annealing as shown in Fig. 2(b). For the measurement session up to

[This article is copyrighted as indicated in the article. Reuse of AIP content is subject to the terms at: http://scitation.aip.org/termsconditions. Downloaded to] IP: 143.107.255.190 On: Wed, 07 Jan 2015 10:43:35

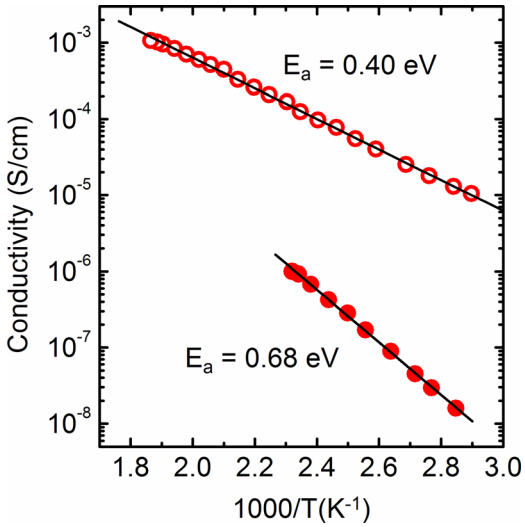

FIG. 3. Arrhenius plot of conductivity during cooling in argon atmosphere obtained after the measurement sessions wherein the temperature was increased up to 160 °C (full circles) and up to 270 °C (open circles).

T = 270 °C, it is also observed that the cooling curve do not follow the heating curve. In this case, the irreversibility indicates that the increase in σ upon heating above 150 °C cannot be entirely described by a simple thermally activated behavior.

From analysis of the Arrhenius plot of Fig. 3, wherein the conductivity data extracted from Fig. 2 is also presented, it is clear that upon cooling, the conductivity of both samples has a thermal activated behavior. Considering that the conductivity follows a simple Arrhenius relation, $\sigma = \sigma_0 \exp(\frac{E_a}{kT})$, both the exponential pre-factor, σ_0, and the activation energy, E_a, change as a result of the heating from 160 to 270 °C. The drop in E_a from 0.68 eV (for the sample heated up to 160 °C) to 0.40 eV (for treatment up to 270 °C) clearly demonstrates that there were significant alterations in the transport mechanism.

In order to obtain further evidences to understand the conductivity results, we have performed XRD, Raman spectroscopy, and EPR measurements in as-prepared H-TNT samples as well as in samples subjected to thermal annealing at 160 °C and at 270 °C, i.e., in annealing conditions similar to those from the electrical measurements. Figure 4 depicts the results from the XRD and Raman experiments.

In the XRD patterns for as prepared H-TNT samples (Fig. 4(a)), contributions from the anatase TiO_2 phase cannot be observed indicating that a complete conversion of the precursor material was achieved. The pattern is typical of H-rich titanate nanotubes and can be assigned to the monoclinic $H_2Ti_3O_7$ structure.[3] For samples subjected to thermal annealing, a weak peak around $2\theta = 42°$ appears in the XRD data, being the relative intensity of this peak slightly higher for the higher T annealing. The appearance of this peak can be attributed to the formation of a small fraction of TiO_2-B phase. This result is consistent with the works of Morgado *et al.* who investigated the crystallographic structure versus annealing temperature for TNTs with different sodium contents[14] and with older studies on bulk titanates.[18] For H-rich samples, changes in the crystalline structure of TNTs that are associated with the appearance of the TiO_2-B phase are only observed for treatments above 300 °C, whereas for higher temperatures (T > 500 °C), a complete transformation to anatase TiO_2 is seen.[4,14,18] However, the unambiguous identification of the TiO_2-B phase by XRD is rather difficult because it yields broad and low intensity reflection peaks.[14] Moreover, the increase in the (110) and (020) reflections for the thermally treated samples might be related to increases in the crystallinity of individual tubes upon heating.

The Raman spectrum of the as prepared samples is typical of H-TNT. It contains major peaks at 280 and 450 cm^{-1} and multiple peaks around 700 cm^{-1} (Fig. 4(b)). The exact assignments of these modes are still matter of discussion. The peak at 280 cm^{-1} can be attributed to vibration modes within TiO_6 octahedra that interact strongly with H^+ counter-ions (H-O-Ti bonds), and the peaks at 450 and 700 cm^{-1} can be attributed to vibration modes between interacting TiO_6 octahedra (Ti-O-Ti bonds).[19–22] The Raman spectra of the annealed samples are very similar to the one of the as-prepared sample, except for an extra peak that appears in the band centered around 700 cm^{-1}. Such change can be associated with a rearrangement of the TiO_6 octahedra due to the removal of OH groups. Such removal results in a decrease in the interlayer gaps and, therefore, in a stronger interaction between adjacent layers.[16,18]

The EPR measurements reveal significant differences among samples treated under argon flow at different temperatures, as can be seen in Figure 5. For H-TNT thermally

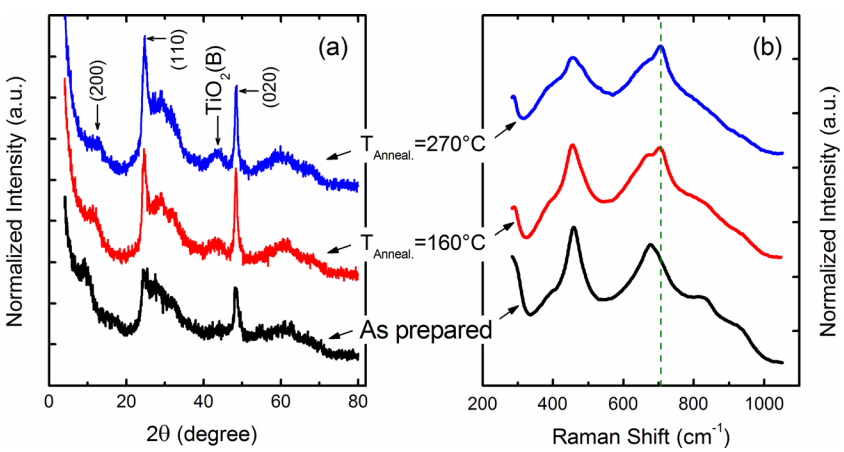

FIG. 4. (a) X-ray diffraction patterns and (b) Raman spectra of as prepared H-TNT (black) and H-TNT subject to thermal annealing at 160 °C (red) and 270 °C (blue).

[This article is copyrighted as indicated in the article. Reuse of AIP content is subject to the terms at: http://scitation.aip.org/termsconditions. Downloaded to] IP: 143.107.255.190 On: Wed, 07 Jan 2015 10:43:35

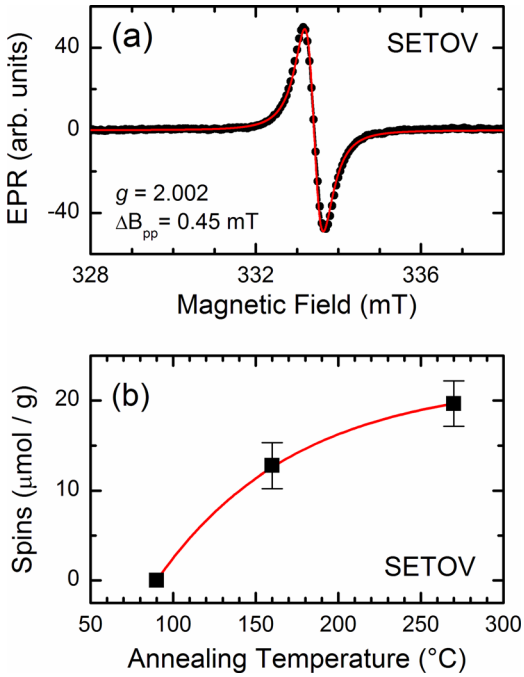

FIG. 5. (a) Electron paramagnetic resonance signal from H-TNT after 270 °C thermal annealing, representing SETOVs. (b) Spin concentration of SETOV as a function of annealing temperature under argon flux.

treated sample at 88 °C, no paramagnetic center was measured, whereas for treatment above 150 °C, an isotropic EPR signal appears having $g = 2.002(1)$ and line width $\Delta B_{pp} = 0.45(5)$ mT, and the intensity of such signal increases with annealing temperature. This signal has been previously observed in titanate nanotubes and was attributed to single-electron-trapped electron oxygen vacancies (SETOVs).[23,24]

The presence of single-occupied oxygen vacancies in slightly reduced TiO_2 crystals has been recognized in infrared and EPR studies[25–27] although the direct identification of oxygen vacancies in TiO_2 nanostructures has proven to be extremely difficult. In nanostructures, oxygen vacancies are believed to act as stabilization centers for oxygen radicals and their existence is indirectly probed through surface charged oxygen radicals (O_2^-, O_2^+, O_2^{2-}) that generate anisotropic EPR signals,[28] which are not seen in the EPR results on H-TNTs reported here. An isotropic EPR signal with g close to the free electron value, similar to the observed in the present work, has also been associated with surface related defects in TiO_2 nanoparticles thermally treated in reducing atmospheres. The isotropic signal indicates the presence of an unpaired electron located in a spherically symmetrical environment, and it has been previously assigned to the localization of a conduction electron in the lattice.[29,30] The existence of oxygen vacancy sites in TiO_2 nanoparticles as stabilizing centers for molecule species suggests that the same site could trap intrinsic charge carriers resulting in SETOVs in titanium oxide based materials, such as the H-TNTs.

The SETOV signal in our samples is relatively stable in air. After 6 months of storage in ambient air, 50% of the initial concentration was still detected. The absolute numbers of such defects can be obtained from a quantitative analysis of the EPR signal comparing with a spin standard and the resulting values for freshly treated TNT samples are shown in Fig. 5(b).

DISCUSSION

Based on the results presented above, it is possible to draw a comprehensive picture of the electrical properties of hydrogen-rich titanate nanotubes. At $T < 100$ °C, electrical transport is dominated by protonic conduction within structural (or physisorbed) water molecules, and conductivity reaches values higher than 10^{-4} S/cm (at $T = 88$ °C). Upon heating up to 150 °C in Ar flow, the structural water is released from the tubular structures, and consequently protonic transport is minimized. Although, for such annealing temperature, defect formation is already observed from EPR, one can consider that H-TNT samples thermally treated at $T = 160$ °C represent an almost pure, dehydrate, $H_2Ti_3O_7$ titanate nanotube phase. This phase has poor electrical conduction ($\sigma \approx 10^{-8}$ S/cm, at $T = 88$ °C) associated with a relatively large activation energy ($E_a = 0.68$ eV). These values are consistent with electronic transport in porous nanocrystalline TiO_2 films, in which the thermal dependence of both the drift mobility and conductivity was found to have similar activation energy values, in the 0.7–0.9 eV range. Such transport is believed to be limited by trapping in surface/inter-grain regions.[31]

For thermal annealing above $T = 150$ °C, the XRD and Raman analysis do not show significant phase change in the titanate nanotube structure, although they provide evidence of subtle structural modifications that can be attributed to the formation of small quantities of the intermediate metastable TiO_2(B) phase. This is consistent with the previous NMR study by Bavikyn *et al.*, who found that for thermal annealing above 140 °C, ion-exchangeable OH groups combine in a non-reversible dehydration reaction that results in a non-stoichiometric phase, as described by the following equation:[16]

$$H_2Ti_3O_7 \rightarrow H_{2(1-z)}Ti_3O_{7-z} + zH_2O. \quad (2)$$

Upon further heating, all OH groups are eventually consumed ($z \rightarrow 1$) and the resulting phase is TiO_2(B), which is an intermediate metastable titanium dioxide phase.[16] Similar dehydration reaction has also been observed in TNT samples annealed under vacuum at 100 °C.[1] Thus, it is reasonable to assume that in the present data set the partial phase transformation [titanate $\rightarrow$ TiO_2(B)] caused by dehydration is detected as changes in the measured conductivity values at $T \geq 150$ °C. The removal of OH groups to form the non-stoichiometric phase $H_{2(1-z)}Ti_3O_{7-z}$ results in oxygen vacancies that act as traps for electrons, forming the SETOV defects observed by EPR at room-temperature.[23]

The presence of oxygen vacancies results in an n-type doping effect that explains the significant increase in the conductivity pre-factor, σ_0, i.e., increase in the density of free carriers, in the sample annealed up to $T = 270$ °C. The question that remains is how the value found for the activation energy upon cooling after a high T annealing ($E_a = 0.40$ eV)

[This article is copyrighted as indicated in the article. Reuse of AIP content is subject to the terms at: http://scitation.aip.org/termsconditions. Downloaded to] IP: 143.107.255.190 On: Wed, 07 Jan 2015 10:43:35

can be correlated to the presence of a high density of oxygen vacancies in the H-TNT. The determination of energy levels associated with oxygen vacancies in TiO_2-based materials has been subject of several studies for decades and it is still an open question.[32] Interestingly, early experimental studies have determined that the thermal ionization energy of single-occupied oxygen vacancies in TiO_2 crystals is similar (0.48 eV) to the activation energy found in this work.[33] More recently, Qian *et al*. have shown that SETOV groups in thermally treated TNTs form a sub-band within the energy band gap, which is 0.68 eV lower than the bottom of the conduction band.[34] However, such value is determined from luminescence measurements, i.e., it is associated with vertical optical transitions, which have energies that are higher than thermal (adiabatic) transitions.[32] Therefore, it is reasonable to attribute the temperature dependence of H-TNT subjected to high T (260 °C) annealing to the thermal ionization energy of single-occupied oxygen vacancies.

CONCLUSION

In conclusion, we have shown that the electrical properties of H-TNT nanotubes have a rich and complicated thermal dependence. It is affected by the presence of intercalated water molecules at low temperatures ($T < 150\,^{\circ}C$) and by the formation of oxygen vacancies due to the dehydration (loss of OH groups) and initial transformation to metastable TiO_2 (B) phase, at higher temperatures ($T > 150\,^{\circ}C$). Overall, we have demonstrated that *in-situ* electrical measurement can be a powerful and sensitive tool to assess subtle structural modifications of nanostructures upon thermal annealing.

ACKNOWLEDGMENTS

This work was supported by CAPES, Fapemig, CNPq, and INCT/Nanomateriais de Carbono. X-ray diffraction measurements were performed at LabCri (DF/UFMG).

[1]T. Kasuga, M. Hiramatsu, A. Hoson, T. Sekino, and K. Niihara, Langmuir **14**, 3160 (1998).
[2]T. Kasuga, Thin Solid Films **496**, 141 (2006).
[3]D. V. Bavykin, J. M. Friedrich, and F. C. Walsh, Adv. Mater. **18**, 2807 (2006).
[4]E. Morgado, Jr., M. A. S. de Abreu, O. R. C. Pravia, B. A. Marinkovic, P. M. Jardim, F. C. Rizzo, and A. S. Araujo, Solid State Sci. **8**, 888 (2006).
[5]D. C. B. Alves, A. M. B. Gonçalves, L. C. Campos, E. S. Avila, R. G. Lacerda, and A. S. Ferlauto, Nanotechnology **22**, 235501 (2011).
[6]D. V. Bavykin, A. A. Lapkin, P. K. Plucinski, J. M. Friedrich, and F. C. Walsh, J. Phys. Chem. B **109**, 19422 (2005).
[7]Z. Chang, J. Liu, X. Sun, and J. Liu, Front. Chem. China **5**, 71 (2010).
[8]M. Yamada, M. Wei, I. Honma, and H. Zhou, Electrochem. Commun. **8**, 1549 (2006).
[9]B. R. Matos, E. I. Santiago, F. C. Fonseca, M. Linardi, V. Lavayen, R. G. Lacerda, L. O. Ladeira, and A. S. Ferlauto, J. Electrochem. Soc. **154**, B1358 (2007).
[10]Y. Jun, H. Zarrin, M. Fowler, and Z. Chen, Int. J. Hydrogen Energy **36**, 6073 (2011).
[11]B. R. Matos, R. A. Isidoro, E. I. Santiago, M. Linardi, A. S. Ferlauto, A. C. Tavares, and F. C. Fonseca, J. Phys. Chem. C **117**, 16863 (2013).
[12]A. Thorne, A. Kruth, D. Tunstall, J. T. S. Irvine, and W. Zhou, J. Phys. Chem. B **109**, 5439 (2005).
[13]W. Hu, L. Li, G. Li, J. Meng, and W. Tong, J. Phys. Chem. C **113**, 16996 (2009).
[14]E. Morgado, Jr., M. A. S. de Abreu, G. T. Moure, B. A. Marinkovic, P. M. Jardim, and A. S. Araujo, Mater. Res. Bull. **42**, 1748 (2007).
[15]F. C. Fonseca and R. Muccilo, Solid State Ionics **166**, 157 (2004).
[16]D. V. Bavykin, M. Carravetta, A. N. Kulak, and F. C. Walsh, Chem. Mater. **22**, 2458 (2010).
[17]P. Cox, *Transition Metal Oxides: An Introduction to Their Electronic Structure and Properties* (Oxford University Press, 2010).
[18]T. P. Feist and P. K. Davies, J. Solid State Chem. **101**, 275 (1992).
[19]Y. Su and M. L. Balmer, J. Phys. Chem. B **104**, 8160 (2000).
[20]S. Bordiga, A. Damin, F. Bonino, G. Ricchiardi, C. Lamberti, and A. Zecchina, Angew. Chem. Int. **41**, 4734 (2002).
[21]A. Gajović, I. Friščić, M. Plodinec, and D. Iveković, J. Mol. Struct. **924–926**, 183 (2009).
[22]B. C. Viana, O. P. Ferreira, A. G. Souza Filho, J. Mendes Filho, and O. L. Alves, J. Braz. Chem. Soc. **20**, 167 (2009).
[23]S. Zhang, W. Li, Z. Jin, J. Yang, J. Zhang, Z. Du, and Z. Zhang, J. Solid State Chem. **177**, 1365 (2004).
[24]J. M. Cho, W. J. Yun, J.-K. Lee, H. S. Lee, W. W. So, S. J. Moon, Y. Jia, H. Kulkarni, and Y. Wu, Appl. Phys. A **88**, 751 (2007).
[25]D. C. Cronemeyer, Phys. Rev. **113**, 1222 (1959).
[26]P. F. Cornaz, J. H. C. van Hooff, F. J. Pluijm, and G. C. A. Schuit, Discuss. Faraday Soc. **41**, 290 (1966).
[27]F. D. Brandão, M. V. B. Pinheiro, G. M. Ribeiro, G. Medeiros-Ribeiro, and K. Krambrock, Phys. Rev. B **80**, 235204 (2009).
[28]E. Carter, A. F. Carley, and D. M. Murphy, J. Phys. Chem. C **111**, 10630 (2007).
[29]E. Serwicka, M. W. Schlierkamp, and R. N. Schindler, Z. Naturforsch., A **36**, 226 (1981).
[30]C. Naccache, P. Meriaudeau, M. Che, and A. J. Tench, J. Trans. Faraday Soc. **67**, 506 (1971).
[31]Th. Dittrich, J. Weidmann, V. Yu Timoshenko, A. A. Petrov, F. Koch, M. G. Lisachenko, and E. Lebedev, Mater. Sci. Eng. B **69–70**, 489 (2000).
[32]P. Deák, B. Aradi, and T. Frauenheim, Phys. Rev. B **86**, 195206 (2012).
[33]A. Ghosh, F. Wakim, and R. Addiss, Phys. Rev. **184**, 979 (1969).
[34]L. Qian, Z. S. Jin, J. W. Zhang, Y. B. Huang, Z. J. Zhang, and Z. L. Du, Appl. Phys. A **80**, 1801 (2005).

[This article is copyrighted as indicated in the article. Reuse of AIP content is subject to the terms at: http://scitation.aip.org/termsconditions. Downloaded to] IP: 143.107.255.190 On: Wed, 07 Jan 2015 10:43:35